Communication—In-Line Detection of Silicon Surface Quality Variation Using Surface Photovoltage and Room Temperature Photoluminescence Measurements

Jae Hyun Kim,[a,b] Seung Min Han,[a] and Woo Sik Yoo[c,*,z]

[a] *Korea Advanced Institute of Science and Technology, Daejeon, 305-701, Korea*
[b] *SK hynix, Inc., Icheon-si, Gyeonggi-do, 467-701, Korea*
[c] *WaferMasters, Inc., San Jose, California 95112, USA*

Occasionally, in volume device manufacturing, a large number of particles may be generated on cleaned Si wafers. Surface (ionic, organic and/or metallic) contamination is generally suspected. However, conventional chemical analysis techniques for contamination are generally not able to distinguish between Si wafers with good and poor particle performance. No suspicious chemicals and elements were detected from any wafers regardless of characterization techniques. Surface photovoltage (SPV) measurement barely showed the differences between wafers with good and poor particle performance. Multiwavelength room temperature photoluminescence (RTPL) showed significant differences in intensity between them, indicating the presence of surface quality variations.
© The Author(s) 2016. Published by ECS. This is an open access article distributed under the terms of the Creative Commons Attribution 4.0 License (CC BY, http://creativecommons.org/licenses/by/4.0/), which permits unrestricted reuse of the work in any medium, provided the original work is properly cited. [DOI: 10.1149/2.0311607jss] All rights reserved.

Manuscript submitted May 16, 2016; revised manuscript received June 14, 2016. Published June 21, 2016.

Contamination related yield loss is a major failure mode in advanced silicon (Si) device volume manufacturing.[1] Silicon wafers are routinely inspected at various stages using in-line and off-line characterization techniques. Incoming wafers are inspected for ionic, inorganic and metal contamination. As device dimensions are shrinking, contamination related device yield loss tends to increase.

Conventional incoming wafer contamination test techniques include ion chromatography (IC) for ionic contamination, gas chromatography with flame ionization detector (GC-FID) for organic contamination and inductive coupled plasma-mass spectroscopy (ICP-MS) for metal contamination.[2–4] Other X-ray techniques, such as total X-ray fluorescence (TXRF) and wavelength dispersive X-ray fluorescence (WDXRF) techniques, are also used as in-line metal contamination techniques.[4] Most techniques have detection limits in the range of ppm ∼ ppb.[2–4] They are not sensitive enough for certain types of process anomalies.

In this study, the root cause of a recent incident generating a large number of particle/defects was investigated using surface photovoltage (SPV)[5] and multiwavelength room temperature photoluminescence (RTPL)[6,7] measurements.

Experimental

Figure 1 shows the flow of Si wafer inspection and process steps. The wafers in front opening shipping boxes (FOSBs) were transferred into front opening unified pods (FOUPs). The wafers were cleaned in deionized (DI) water and the surface inspected for particles and defects. Typically, all wafers pass the inspection. Silicon dioxide (SiO_2) films were deposited on 300 mm Si (100) wafers in a plasma enhanced chemical deposition (PECVD) system using liquid tetraethyl orthosilicate (TEOS: $Si(OC_2H_5)_4$) as a source of Si. The Si wafers with PECVD SiO_2 films were inspected for particles and defects again.

Three batches (A, B and C) of 25 Si wafers ($3 \times 25 = 75$ wafers) with native oxide (SiO_2/Si) were allocated for this study. Four wafers per batch were used for chemical analyses (IC for ionic contamination, GC-FID for organic contamination and ICP-MS for metal contamination). For SPV measurements, the contact potential difference (or probe potential), V_{cpd}, was mapped under green light-emitting-diode (LED) illumination at a peak wavelength of 524 nm. RTPL measurements, intensity and spectral distribution from the Si wafers, were mapped in the wavelength range of 900 ∼ 1400 nm under 650 and 827 nm excitation with penetration depths of ∼4.0 and ∼10 μm.[6,7] Both SPV and RTPL mapping was done on five wafers per batch in detail (>15,000 points per wafer). The rest of the wafers (11 wafers per batch) were used for TEOS oxide deposition for particle/defect performance verifications.

Results and Discussion

All three batches of Si wafers showed identical results within measurement errors. No suspicious ions, organics and elements were detected. The routine chemical analysis techniques could not discriminate one batch from the others. The detection limits of ICP-MS for most metallic elements on 300 mm Si wafer surface are in the range of ppb ∼ ppt (or down to 10^{10} cm^{-2}). GC-FID is used for hydrocarbon contamination analysis in the range of 5 ∼ 1 ppm. IC can detect anions and cations in the level of 20 ∼ 1 ppb.

The particle/defect inspection results on Si wafers only from batches A and B after PECVD TEOS oxide film deposition showed a very high number of particle/defect (>120 nm in diameter) count range of 3,000 ∼ 40,000 per wafer. The wafers from batch C showed a very small number of particle/defect counts, typically below 5 per wafer.

Average contact potential difference (V_{cpd}) values from detailed SPV mapping results and average RTPL intensity values from detailed RTPL mapping under 650 nm and 827 nm excitations are shown in Fig. 2a. Both RTPL intensity under different excitation wavelengths and intensity ratio between them were more sensitive than the

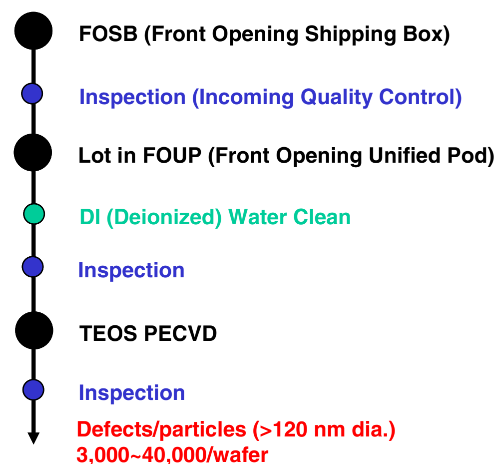

Figure 1. Various inspection points from wafer start.

*Electrochemical Society Member.
zE-mail: woosik.yoo@wafermasters.com

Downloaded on 2017-05-29 to IP 143.248.123.117 address. Redistribution subject to ECS terms of use (see ecsdl.org/site/terms_use) unless CC License in place (see abstract).

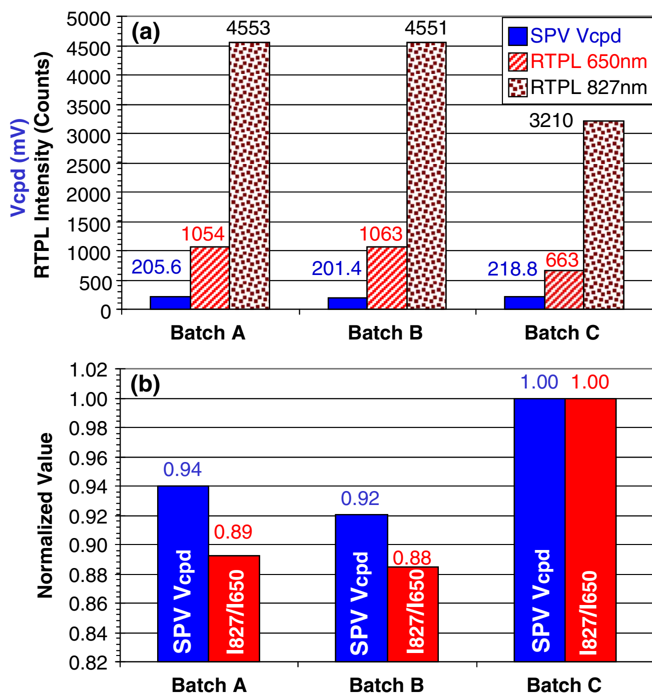

Figure 2. (a) average and (b) normalized V_{cpd} and RTPL intensity ratio (I_{827}/I_{650}) values over three 5-wafer batches (3 batches: 15 new blanket Si wafers).

variations in V_{cpd} values between different batches of Si wafers. For easy comparison, normalized average V_{cpd} values and RTPL intensity ratio (I_{827}/I_{650}) values on five wafers in each batch are plotted in Fig. 2b. The trends of V_{cpd} values and RTPL intensity ratio (I_{827}/I_{650}) values on Si wafers from batches A, B and C are the same while the variations between the batches are higher in the RTPL intensity ratio (I_{827}/I_{650}).

Average V_{cpd} was slightly (7.0%) lower (203.5 mV) for the wafers from batch A and B compared to the values (218.8 mV) for the wafers from batch C. The V_{cpd} difference between batches was very small (15.3 mV). SPV maps (not shown) indicated slightly higher V_{cpd} values near the edge of the wafers indicating possible differences in SiO_2/Si interface quality and/or electronic states.

The RTPL intensity maps showed very strong correlation with the particle/defect performance after PECVD TEOS oxide deposition (Fig. 3). The RTPL intensity of Si wafers from the batches A and B were significantly (approximately 41.8%: 4,551 counts vs. 3,210 counts) higher than Si wafers from batch C. The RTPL maps for wafers from the batches A and B showed localized intensity increase near the contact points with FOSB materials, suggesting possible contamination. The RTPL maps for the wafers from batch C did not show the localized intensity increase near the contact points. A wafer (Slot 22) from batch C showed possible dopant concentration variations and non uniformity due to the wafer cutting location in a Si ingot.

RTPL studies showed very high sensitivity to surface passivation, native oxide/Si interface quality,[6] dielectrics/Si interface quality,[7] plasma induced damage (PID),[8] etching damage,[9] ultraviolet (UV) induced damage,[10] X-ray induced radiation damage,[11] implant damage,[12,13] metal contamination,[6] minority carrier lifetime.[14] An RTPL study on intentionally iron (Fe) contaminated lightly doped p-type and n-type Si wafers with Fe contamination ranged from 10^9 cm^{-3} to 10^{12} cm^{-3} showed good correlation between photoconductance decay (PCD) lifetime, SPV diffusion length (DL) and iron readings.[15] RTPL was reported to be sensitive to iron contamination at concentrations exceeding 10^{10} cm^{-3} (<ppb) as calibrated by SPV using lightly doped p-type silicon.

Figure 4a shows spectral distribution of excitation light source for SPV and RTPL measurements used in this study. Similarities and differences of SPV and RTPL are schematically illustrated using an energy band diagram in Fig. 4b. Both techniques use high energy (E_{exe} > E_{gap} = 1.12 eV) photons to generate electron-hole (e - h) pairs. As the e - h pairs are separated by built-in potential near the surface, band bending occurs. The amount of band bending is determined by the balance between surface charge density and electrically active surface/interface state density. SPV electrically measures the change

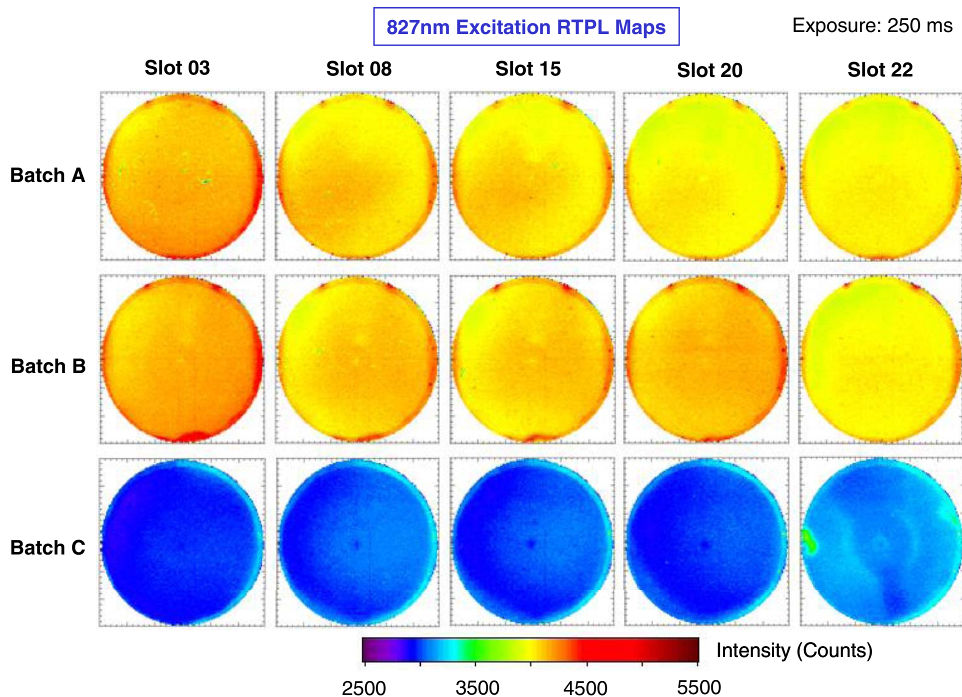

Figure 3. 827 nm excited RTPL intensity wafer maps of 15 new blanket Si wafers.

Downloaded on 2017-05-29 to IP 143.248.123.117 address. Redistribution subject to ECS terms of use (see ecsdl.org/site/terms_use) unless CC License in place (see abstract).

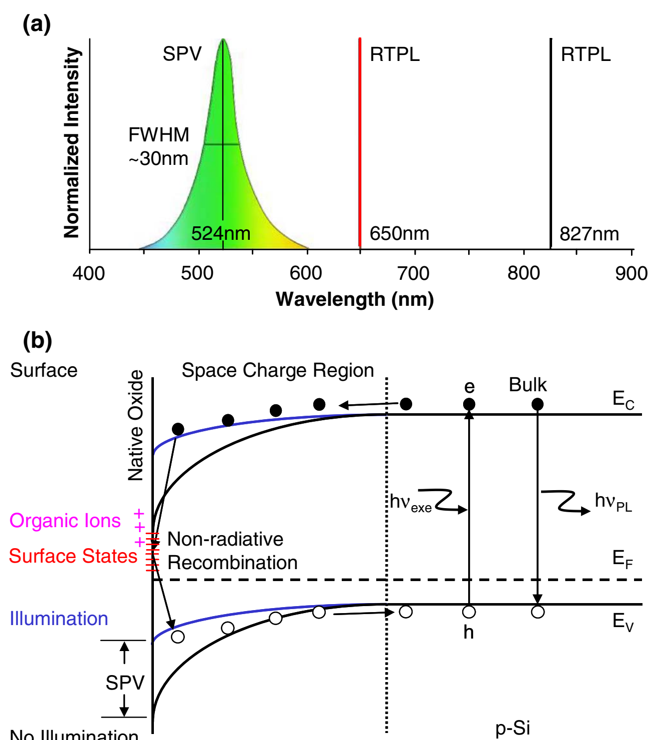

Figure 4. (a) spectral distribution of excitation light source and (b) schematic illustration of band bending with and without illumination. ($h\nu_{exe}$: photon energy for excitation and $h\nu_{PL}$: photon energy for photoluminescence).

in band bending (V_{cpd}) by illumination. RTPL optically measures the intensity and spectral distribution of photons emitted from Si. SPV phenomenon also occurs during RTPL measurements.

The SPV technique utilizes the change of the electrochemical potential in the space-charge region(s) of a semiconductor during excess carrier generation due to illumination of the sample. In wavelength dependence SPV(λ), it probes diffusion of carriers in the bulk Si and the surface properties is inferred by linear regression. However, the sensitivity required in advanced device manufacturing cannot be met.[16] RTPL is a fast and non-contact characterization technique to measure passivation and surface recombination of Si during or after processing/modification of Si surfaces at RT.[16,17] The integrated RTPL intensity is inversely proportional to the amount of non-radiative recombination centers.[18]

A low level (350 ng/cm^{-2}) of pentanoic acid (formula: $C_{16}H_{30}O_4$) out gassing was detected from FOSBs (made of polycarbonate and thermoplastic elastomer) for the batch A and B with particle issues by GC-MS (gas chromatography-mass spectroscopy).

Higher surface state sensitivity and spatial resolution required in advanced device manufacturing can be realized by multiwavelength RTPL measurements (Fig. 2 and Fig. 3). Si wafers with native oxide give very weak RTPL signal due to the high density of electrically active surface/interface states which act as non-radiative recombination centers. Clean Si wafers (Batch C) with native oxide layer has high density of electrically active surface/interface states and give lower RTPL signal. When the Si surface or native oxide/Si interface is passivated by chemicals (including very small amount of organic ions from FOSB materials) or hydrogen, the density of electrically active surface/interface states decrease and RTPL intensity is increased.

Summary

Conventional chemical analysis (IC, GC-FID and ICP-MS) techniques were not able to distinguish between Si wafers with good and poor particle performance the TEOS oxide PECVD process in device volume manufacturing. No suspicious ions, organic residues and metallic elements were detected from all wafers, regardless of characterization techniques. Very small amounts of surface contamination, below detection limits of conventional contamination analysis techniques, are strongly suspected. SPV measurements barely detect the difference in surface potentials between wafers. Multiwavelength RTPL showed significant (up to 41.8%) differences in intensity between good and poor wafers, a strong indication of the presence of surface quality variations between them.

References

1. S. De Gendt, D. M. Knotter, K. Kenis, P. W. Mertens, and M. M. Heyns, *J. Electrochem. Soc.*, **154**(11), H977 (2007).
2. http://www.mee-inc.com/hamm/ion-chromatography-ic/.
3. http://www.sepscience.com/Techniques/GC/Articles/208-/GC-Solutions-11-The-Flame-Ionization-Detector.
4. http://www.eag.com/mc/analytical-techniques.html.
5. D. K. Schroder, *Materials Science and Engineering: B*, **91–92**, 196 (2002).
6. S. K. Jang Jian, C. C. Jeng, and W. S. Yoo, *AIP Advances*, **2**, 042164 (2012).
7. W. S. Yoo, B. G. Kim, S. W. Jin, T. Ishigaki, and K. Kang, *ECS J. Solid State Sci. Technol.*, **3**(11), N142 (2014).
8. J. G. Kim, H. J. Cho, S. K. Park, S.-H. Lee, B. G. Choi, J. Y. An, Y. I. Cheon, Y. H. Jeon, T. Ishigaki, K. Kang, and W. S. Yoo, *ECS J. Solid State Lett.*, **3**(3), N11 (2014).
9. S. K. Jang Jian, C. C Jeng, T. C. Wang, C. M. Huang, Y. L. Wang, and W. S. Yoo, *ECS J. Solid State Sci. Technol.*, **2**(5), P214 (2013).
10. J. G. Kim, H. J. Cho, S. K. Park, S. -H. Lee, B. G. Choi, J. Y. An, Y. I. Cheon, Y. H. Jeon, T. Ishigaki, K. Kang, and W. S. Yoo, *ECS J. Solid State Lett.*, **3**(3), N11 (2014).
11. J. H. Kim, J. Y. Park, C. H. Lee, Y. J. Yoon, J. S. Yoo, T. Ishigaki, K. Kang, and W. S. Yoo, *J. Vac. Sci. Technol. B*, **34**, 041208 (2016).
12. W. S. Yoo, B. S. Jeon, S. D. Kim, T. Ishigaki, and K. Kang, *ECS J. Solid State Sci. Technol.*, **4**(12), P436 (2015).
13. W. S. Yoo, M. Yoshimoto, A. Sagara, and S. Shibata, *ECS J. Solid State Lett.*, **4**(8), P51 (2015).
14. D. H. Baek, S. B. Kim, and D. K. Schroder, *J. Appl. Phys.*, **104**, 054503 (2008).
15. I. Rapoport, P. Taylor, B. Orschel, J. Kearns, F. Kirscht, A. Buczkowski, and S. Hummel, *AIP Conf. Proc.*, **772**, 103 (2005).
16. E. Kamieniecki, *ECS Proceedings*, **PV 99-16**, 259 (1999).
17. F. Yang, R. Hunger, K. Rademann, and J. Rappich, *Phys. Ststus Solidi C*, **7**, 161 (2010).
18. https://www.helmholtz-berlin.de/forschung/oe/ee/si-pv/arbeitsgebiete/heteroemittersolarzellen/charakterisierungsmethoden/photolumineszenz_en.html.

Downloaded on 2017-05-29 to IP **143.248.123.117** address. Redistribution subject to ECS terms of use (see **ecsdl.org/site/terms_use**) unless CC License in place (see abstract).